Integrity Assessment of Pipeline Systems by an Enhanced Indentation Technique

Gabriella Bolzon, Ph.D.[1]; Giovanna Gabetta[2]; and Bernardo J. Molinas, Ph.D.[3]

Introduction

A high and rising number of pipelines deliver significant volumes of hydrocarbons worldwide, in particular in the Mediterranean area. If well-constructed, carefully monitored, and properly maintained, pipeline systems constitute safe and environmentally sound means of transportation. However, aging of existing networks represents a growing and challenging problem in the oil sector while responsibility and awareness about environmental protection is increasing. Thus, procedures and practices for reliable and fast integrity assessment of pipeline systems during their whole lifetime are highly demanded.

Material aging and environmentally assisted cracking induce degradation of the steel properties and affect important material characteristics such as residual strength [e.g., Jang et al. (2005b), Bolzon et al. (2011a), Seok and Koo (2006), Nykyforchyn et al. (2010) and references therein]. The evolution of the damaging processes is usually evaluated on specimens extracted from spools removed from components after service. The development of alternative, less-invasive methods is promoted by the growing demand for the continuous monitoring of oil transportation systems exposed to long-term exploitation for retrofitting and requalification purposes.

Instrumented indentation has been proposed as a nondestructive testing (NDT) methodology for the diagnosis of material degradation both in laboratory applications and in structural components. The operative procedure implemented by Jang et al. (2005a) for the assessment of pipeline safety is based on the collection of data from multiple loading–unloading sequences carried out at about 1.5-kN maximum force, producing the penetration of a spherical tip on the component surface for about 150-μm depth. The results are analyzed in light of some a priori knowledge on the target material characteristics to recover the material response in terms of representative stress and representative strain measures (Qian et al. 2007) and to avoid possible misinterpretation (Chen et al. 2007).

Parameter estimation of enhanced reliability results from the alternative approach proposed by Bolzon et al. (2004), which acquires the geometry of the imprint left on the surface of the tested material sample and exploits this information with an inverse analysis tool for mechanical characterization purposes. Geometrical data may even replace the loading–unloading indentation curves, and simple hardness testers can be used for the identification of material properties (Bolzon et al. 2011b). A number of validation studies performed on metals and alloys subjected to Rockwell indentation or hardness test [ASTM E18–11 (ASTM 2011a); EN ISO 6508–1 (EN ISO 2005)] at about 2-kN maximum force confirm that the identified material properties are consistent with those of standard tensile tests (Bolzon et al. 2012). The material volume involved by indentation at the prescribed load level is in fact representative of the bulk characteristics, whereas surface effects are minimized by the conical shape of the tip.

Portable instruments and powerful small computers allow one to perform the experiments and process the acquired information directly on site. Instrumented indenters can be equipped with anchorages specifically designed for pipelines (e.g., the apparatus shown in Fig. 1), whereas microscopes with variable focal distance and minimum encumbrance return the geometry of the imprint left on the material surface, as shown, for instance, in Fig. 2. The collected data can be exploited for material characterization purposes with the aid of a simulation model of the experiment according to the identification procedure schematized by the flow chart of Fig. 3 in a spreading approach envisaged by the ISO/TR 29381 (ISO 2008). The parameter values that minimize the discrepancy between measurements and the results of the simulation model are assumed to be constitutive properties. Calculations are sped up with no significant accuracy loss by means of model reduction techniques described, e.g., by Bolzon and Buljak (2011) and Bolzon and Talassi (2012). Thus, the mechanical characteristics of the investigated material can be determined in almost real time.

The reliability of this methodology has been verified on a spool extracted from Meleiha–El Hamra pipeline (Abdou 2013) after about 25 years of service. The output of this case study permits

[1]Associate Professor, Dept. of Civil and Environmental Engineering, Politecnico di Milano, Piazza Leonardo da Vinci 32, 20133 Milano, Italy (corresponding author). E-mail: gabriella.bolzon@polimi.it

[2]Senior System Engineer, eni E&P Division, ISTAC, Via Emilia 1, 20097 San Donato Milanese (MI), Italy. E-mail: giovanna.gabetta@eni.com

[3]Researcher and Project Manager, VeneziaTecnologie S.p.A., Via delle Industrie 39, 30175 Porto Marghera (VE), Italy. E-mail: bmolinas@veneziatecnologie.it

Note. This manuscript was submitted on February 3, 2014; approved on June 19, 2014; published online on July 30, 2014. Discussion period open until December 30, 2014; separate discussions must be submitted for individual papers.

Fig. 1. Anchorage of an indenter system on the external surface of a pipe

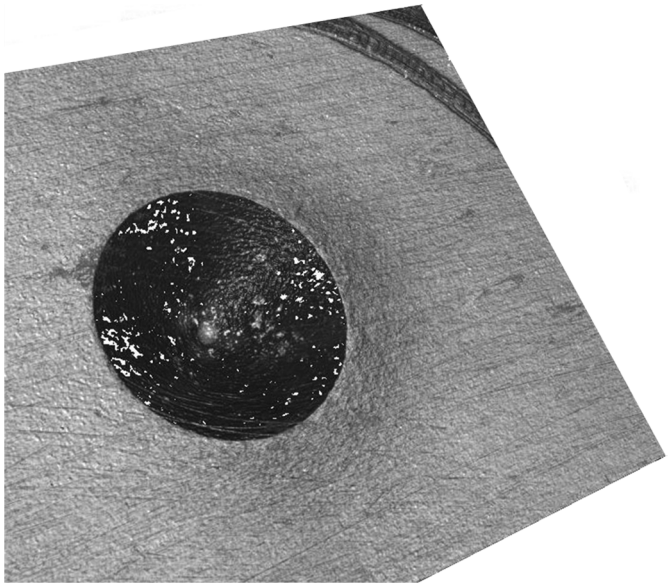

Fig. 2. Residual imprint left on the pipe surface by Rockwell indentation: optical measurement of the coordinates of the deformed surface is performed by a portable microscopy system with variable focal distance

one to draw some general conclusions on the possibility of performing effective integrity assessment of pipeline systems on site during their whole lifetime.

Case Study

The buried pipeline (165.2 km long) carrying crude oil from Meleiha to El Hamra across the Egyptian desert was commissioned in 1985. The pipe is made of steel grade X52 according to API 5L (American Petroleum Institute 2004) specification. The altimetry shows less than 250-m altitude decrease in the line length. The pipe, 406.4-mm (16-in.) diameter and 9.53-mm (0.375-in.) thickness, operates at 6.6 MPa (66 bar, 960 psig) pressure with a flow rate of about 19,000 m^3/day (120,000 bbl/day). Stabilized oil with very low water cut (less than 2%) and gas content is transported. Thus, the pipeline is at very low risk of internal degradation: a corrosion rate lower than 0.05 mm/year along the whole length is predicted by the popular (in oil industry) semiempirical model developed by de Waard et al. (1995).

A spool was extracted from the top of the line after a hot-tapping operation carried out according to the recommendations of the U.S. Environmental Protection Agency (2006). The spool surfaces were polished and prepared following the indications provided by ISO 14577–1 (ISO 2002). Instrumented indentation was performed applying 2-kN maximum force by a sphero-conical (Rockwell) tip, conforming with standards for structural applications: 120° opening angle and spherical end with 200-μm radius [ASTM E18–11 (ASTM 2011a); EN ISO 6508–1 (EN ISO 2005)]. The tip is made of diamond, with typical elastic modulus 1,140 GPa and lateral contraction ratio 0.07. The force exerted on the spool during the indentation test was monitored during the loading and unloading phases as a function of the penetration depth of the tip. The geometry of the residual imprint left on the metal surface was finally acquired at the removal of the indentation tool.

The information gathered from the experiments was exploited in the inverse analysis procedure schematized in Fig. 3. The constitutive properties were inferred from the minimization of the discrepancy between the measurements collected during the test and the output of a reliable model of the experiment. Details can be found in Bolzon et al. (2012) and in references therein.

In the present case, the indentation test was simulated by the finite-element method in a large strain, large displacement regime. The metal response was assumed to be isotropic, represented by the associative Huber–Hencky–von Mises (HHM) constitutive law with exponential hardening rule beyond the initial linear elastic range, defined by the limit

$$\sigma_{eq} \leq \sigma^Y \left(\frac{E\varepsilon_{eq}}{\sigma^Y} \right)^n \tag{1}$$

where the equivalent stress and plastic strain measures, indicated by σ_{eq} and ε_{eq}, respectively, depend as follows on the deviatoric part $\boldsymbol{\sigma}'$ of the "true" stress tensor $\boldsymbol{\sigma}$ and on the plastic component $\boldsymbol{\varepsilon}'^p$ of the logarithmic strains collected in tensor $\boldsymbol{\varepsilon}$:

$$\sigma_{eq} = \sqrt{\frac{3}{2}\boldsymbol{\sigma}':\boldsymbol{\sigma}'}, \qquad \varepsilon_{eq} = \sqrt{\frac{2}{3}\boldsymbol{\varepsilon}'^p:\boldsymbol{\varepsilon}'^p} \tag{2}$$

Young's modulus E, the initial yield limit σ^Y, and the hardening exponent n entering Eq. (1), represent the "true" parameters to be recovered from the experimental results.

Nominal values of material properties of engineering interest, like the tensile strength, are inferred assuming that plastic deformation develops at constant volume, consistently with HHM assumptions. "True" and nominal uniaxial tensile stress–strain curves are shown in Fig. 4.

The actual mechanical characteristics of the material were determined also by means of tension tests carried out according to EN ISO 6892–1 standards (European Committee for Standardization 2009) on specimens worked out from the pipe thickness (Fig. 5).

Experimental Results

The curves drawn in Fig. 6 constitute the output of the indenter shown in Fig. 1 applied to the external (Y) and internal (Z) surfaces of the spool, prepared according to ISO 14577–1 (ISO 2002). Notice the repeatability of the data acquired in position Z.

The geometry of the residual deformation left on the component by the Rockwell tip was mapped by a portable microscope with variable focal distance. Fig. 7(a) visualizes one typical instrumental

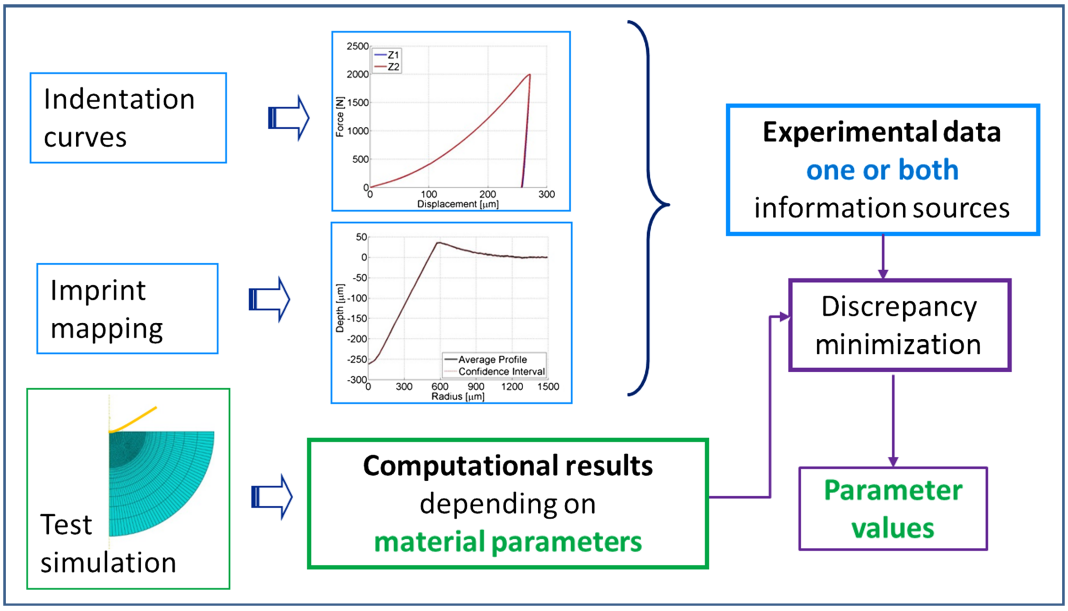

Fig. 3. Outline of the material characterization procedure

output, consisting of a large set of coordinates (x, y, z). This information is processed to retrieve the mean profile and the confidence interval represented in Fig. 7(b), defined by the points over eight radial directions at 45° angular distance on the deformed surface. The confidence interval is hardly visible because of the extremely low data dispersion, which reflects the isotropy of the material response under the axis–symmetric tip and the accuracy of the measurement system.

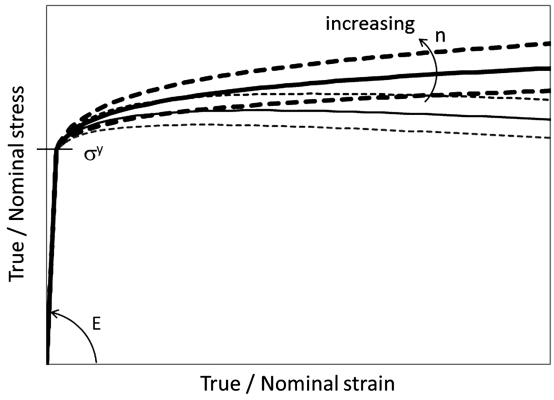

Fig. 4. True (thick lines) and nominal (thin lines) corresponding tensile stress–strain curves for fixed elastic modulus E and initial yield limit σ^Y and increasing hardening exponent n

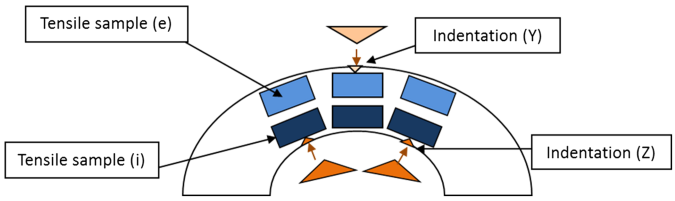

Fig. 5. Sketch of the cross section of the pipe with the tested material zones

Either all collected information or only geometrical data have been used to recover the actual values of the constitutive parameters. More specifically, $N_h = 100$ values h_{mi} (subscript m indicates measurement and $i = 1,2, \ldots, N_h$) of the tip penetration depth were sampled at 50 equal increments of the force along the loading and the unloading branches of the indentation curves shown in Fig. 6. The mean profile of the residual imprints, shown, for instance, in Fig. 7(b), was described by $N_u = 100$ displacement components u_{mj} ($j = 1,2, \ldots, N_u$) measured orthogonally to the initial flat surface of the sample at equidistanced radial points. The corresponding quantities $h_{ci}(\mathbf{z})$ and $u_{cj}(\mathbf{z})$ (subscript c means computed) were evaluated by a computational model of the experiment, described in detail by Bolzon et al. (2012) and based on finite-element simulations carried out by a commercial code (Simulia Dassault Système 2009). The numerical output depends on the parameters that represent the sought material characteristics (namely E, σ^Y, and n in the present context) collected by the vector $\mathbf{z}$. The optimum $\mathbf{z}$ entries were recovered by the minimization of a discrepancy function, defined as

$$\omega(\mathbf{z}) = \alpha \sum_{i=1}^{N_h} \left[\frac{h_{mi} - h_{ci}(\mathbf{z})}{h_{\max}}\right]^2 + \sum_{j=1}^{N_u} \left[\frac{u_{mj} - u_{cj}(\mathbf{z})}{u_{\max}}\right]^2 \qquad (3)$$

In the preceding relationship, $h_{\max}$ and $u_{\max}$ represent two normalization terms, assumed to coincide with the maximum penetration depth experienced during the test and with the largest residual deformation left on the indented surface, respectively. Factor α was null when parameter identification was based on imprint data only; α assumed unit value when all available information was taken into account.

The minimization of the discrepancy function [Eq. (3)] was performed by a robust first-order iterative algorithm (“Trust Region”) available in popular optimization toolboxes (Math Works 2007). In some cases, the elastic modulus was fixed to the value of 205 GPa, typical of the considered pipeline steel, to reduce the computational burden of the minimum search.

The optimum values of σ^Y, n, and (possibly) E returned by the preceding outlined inverse analysis procedure permit one to reproduce the experimental output with the accuracy shown, for

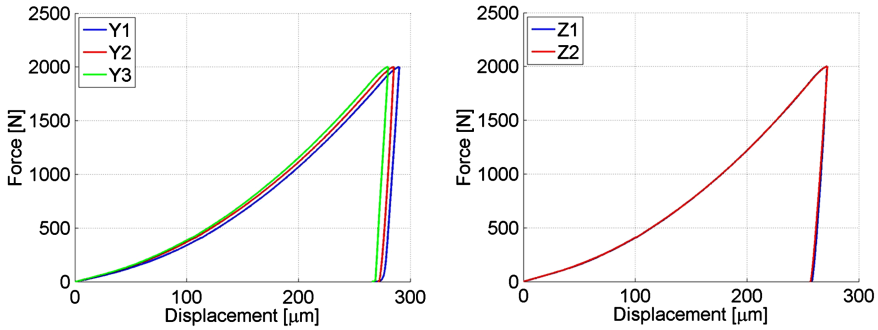

Fig. 6. Indentation curves relevant to the external (Y) and internal (Z) surface of the pipe

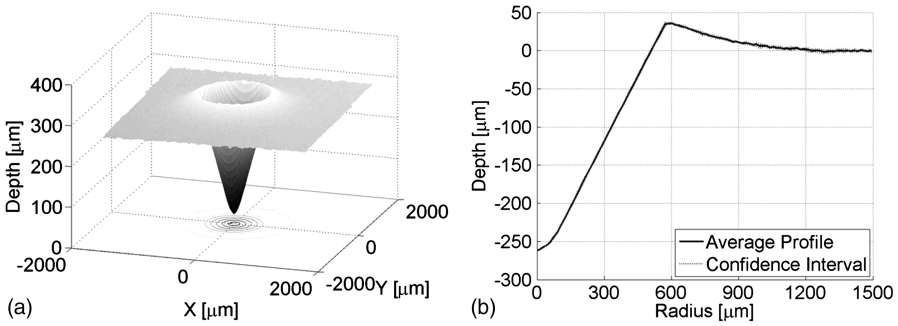

Fig. 7. Typical imprint left on the indented surfaces: (a) three-dimensional reconstruction of the geometry; (b) average profile with the corresponding confidence interval

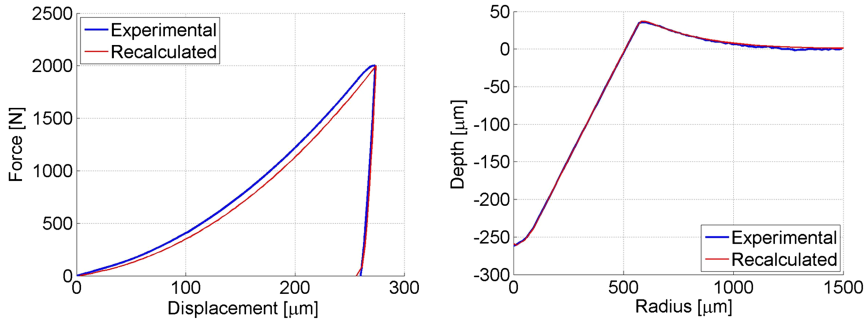

Fig. 8. Comparison between the experimental information collected from indentation (position Z) and the corresponding output of the numerical simulation of the test performed with the identified material parameter set

instance, in Fig. 8; simulation is performed with the constitutive parameter set identified on the basis of the data relevant to the imprint geometry only. The fair agreement between experimental and recalculated indentation curves supports the reliability of this approach.

Tables 1 and 2 summarize the nominal values of the material properties, which were inferred from the identified parameters assuming that plastic deformation occurs at constant volume, consistently with HHM assumptions.

Tensile tests were also performed, for comparison purposes, on $4 + 4$ specimens cut in pairs parallel to the longitudinal axis of the pipeline in positions close to either the internal or the external surface, as shown in Fig. 5. The geometry of the samples, with $4 \times 8\text{-mm}^2$ transversal cross section, is consistent with the requirements

Table 1. Mechanical Properties from Indentation Curves and Imprint Geometry (Nominal Values)

Zone	Value	Elastic modulus (GPa)	Yield limit (MPa)	Tensile strength (MPa)
External (Y)	Mean	225	359	539
	Standard deviation	20	9	6
Internal (Z)	Mean	231	455	571
	Standard deviation	22	73	11

Table 2. Mechanical Properties from Imprint Geometry (Nominal Values)

Zone	Value	Yield limit (MPa)	Tensile strength (MPa)
External (Y)	Mean	360	527
	Standard deviation	18	13
Internal (Z)	Mean	432	575
	Standard deviation	22	7

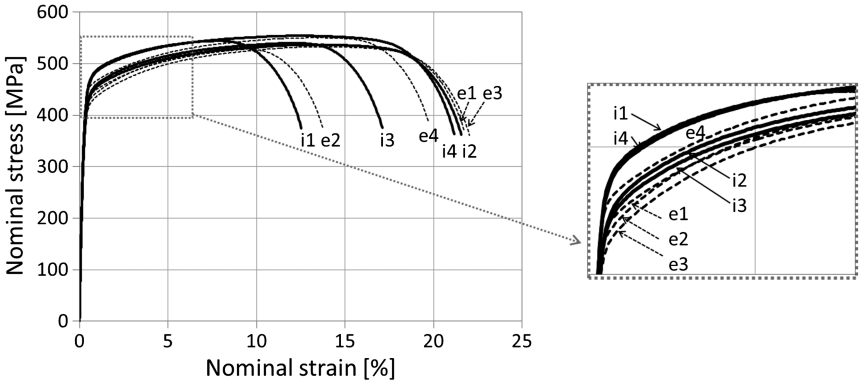

Fig. 9. Output of the tensile tests: specimens "i" and "e"

of EN ISO 6892–1 (European Committee for Standardization 2009). The resulting nominal stress versus nominal strain curves are reported in Fig. 9. Thin dashed lines refer to "e" (external) specimens; whereas continuous lines represent the mechanical response of "i" (internal) specimens. Most curves concerning i specimens lie below those relevant to e samples. The average values of the sought material properties are summarized in Table 3 with the corresponding standard deviation.

Discussion

The discrepancy among the properties reported in Table 3 concerning e and i tensile specimens falls within the statistical dispersion of data and suggests that the material characteristics in the investigated spool are nearly uniform across the thickness. This outcome could be somewhat anticipated, because no significant damage accumulation is expected in this line, which transports stabilized oil in almost uniform flow regime along its whole length. Furthermore, the considered material portion was extracted from the top of the component; whereas degradation is generally higher in the down-internal parts of the pipe, due to the combined effect of the water accumulated at the pipe bottom and of the hydrogen produced by corrosion reactions and absorbed by the metal.

However, the experimental results summarized by the curves drawn in Fig. 9 show that the tensile strength of the internal samples is systematically higher than that exhibited by the external ones; whereas the failure strain is mostly lower. These features may reflect some material hardening induced by the fabrication method of the pipe, but the spatial definition allowed by tensile specimens leaves this conjecture rather indeterminate.

On the contrary, the mechanical properties inferred from indentation (reported in Tables 1 and 2) evidence a clear gradient in the material characteristics from the external to the internal surface of the tube, although average values substantially conform with the outcome of the more traditional methodology based on tensile tests. Results are summarized in Table 4.

Table 3. Mechanical Properties from Tensile Test (Nominal Values)

Zone	Value	Elastic modulus (GPa)	Yield limit (MPa)	Tensile strength (MPa)	Failure strain (%)
External (e)	Mean	214	418	537	19.2
	Standard deviation	15	15	9	3.8
Internal (i)	Mean	198	418	543	18.0
	Standard deviation	7	15	7	4.2

The precision of the performed measures, evaluated according to ISO 5725–1 (ISO 1994) as the ratio between the standard deviation and the mean value of the mechanical properties of interest, is reported in Table 5. Precision values of either tensile and indentation test are comparable.

Clearly, neither test constitutes an absolute measurement system in the present context because the material volume involved by the experiments is rather different: in one case, sample dimensions are comparable with the pipe thickness; in the other, the load affects some hundred micrometers material depth only. This dimension, although small, is one order-of-magnitude higher than the grain size (between 10 and 30 μm) of pipeline steel, and a large number of grains are therefore engaged in the deformation.

Grain boundaries are clearly visible in the micrograph of Fig. 10, which concerns API X52 pipeline steel. The material morphology is evidenced by an appropriate etching of the lapped and polished surface. The average grain size can be determined by means of the methodologies suggested by ASTM (2013) standards on specimens prepared according to ASTM (2011b). The so-called "Intercept Procedures," which involve the actual count of the number of grains intercepted by a test line and of the number of grain boundary intersections with a test line, has been primarily used.

A simple computation of the number of grains and of the grain boundary surface contained in the volume of the residual imprint can be performed (Molinas and Povolo 1992) by a cubic idealization of the grain shape and by the schematization of the indenter tip as a cone with 120° opening angle. With these assumptions and 250-μm penetration depth, roughly indicated by the curves in Fig. 6 and by the profile in Fig. 7, the estimated number of grains is between 2,000 and 50,000, and the extension of the grain boundaries

Table 4. Sequence of the Identified Parameter Values from the External to the Internal Surface of the Pipe

Mechanical property	Imprint (Y) – tensile test (e) – tensile test (i) – imprint (Z)
Yield limit (MPa)	$360 < 418 = 418 < 432$
Tensile strength (MPa)	$527 < 537 \approx 543 < 575$

Table 5. Measurement Precision

Mechanical property	Tensile test (e)	Tensile test (i)	Imprint (Y)	Imprint (Z)
Yield limit (%)	3.6	3.6	5.0	5.1
Tensile strength (%)	1.7	1.3	2.5	1.2

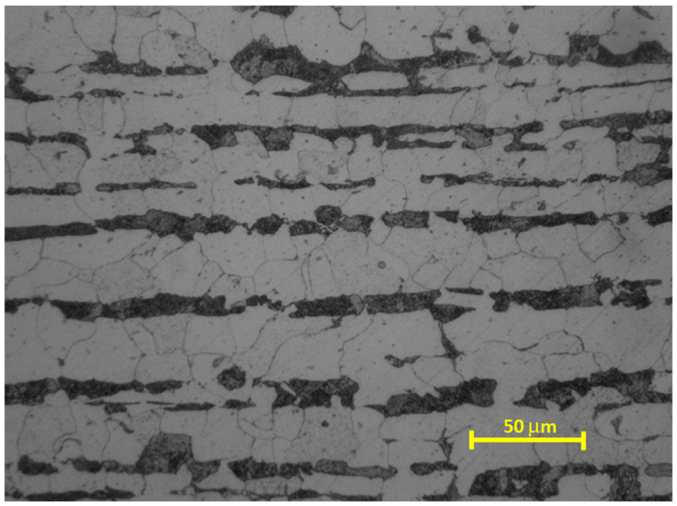

Fig. 10. Morphology of API X52 pipeline steel (optical micrograph)

surface is between 7 and 22 times the contact area of the imprint with average grain size 30 and 10 μm, respectively. The total number of grains and the extension of the grain boundary surface affected by indentation are actually much higher.

The micrograph of Fig. 10 shows that API X52 material phases are arranged along narrow bands, a few or tens of micrometers wide, smaller or much smaller than the side dimensions of the volume sampled by the indenter tip. The results presented herein can therefore be considered truly representative of the macroscopic material response also in this respect, and the envisaged methodology can be applied to other pipeline materials with even more favorable morphology (for example, API X100).

Conclusions

The mechanical properties of pipeline steel have been evaluated starting from the experimental information collected from a NDT based on indentation. Results have been compared with the output of more traditional tests performed on standard tensile specimens cut from the thickness of the pipe. Although the average values match, a deeper insight on the distribution of the material characteristics across the component has been gained from indentation, which represents a suitable tool for the determination of occasional gradients that cannot be revealed with the same accuracy by tensile tests.

Indentation techniques are fast, rather inexpensive, and noninvasive at the scale of structural components like the investigated pipe. This NDT can be easily repeated, allowing a statistical characterization of the results even on small material portions.

The reliability of the identified parameters is enhanced in the proposed approach by geometrical data. The presented results and the outcome of laboratory studies carried out on different metals and alloys show that the performances of material characterization techniques resting on the geometry of the imprint left on the indented area are rather interesting in terms of reduced dispersion and representativeness of the results and according to standard evaluation criteria in metallurgy.

Indentation techniques permit one to perform measurements in the field, on operating components, because material extraction to work out specimens is not required. Material properties can be recovered almost in real time, speeding up calculations by model reduction techniques, which do not significantly affect accuracy. Details are not provided here but can be found in the quoted literature (Bolzon and Buljak 2011; Bolzon and Talassi 2012).

The results of the considered methodology can be exploited for structural diagnosis purposes provided that the external material layer is representative of the bulk. These features make this NDT suitable for effective integrity assessment of pipeline systems during their whole lifetime.

Acknowledgments

The authors of this communication wish to thank A. Zuppello (eni Group) for providing the examined spool and information about the pipeline.

References

Abdou, H. A. M. (2013). "Case study in upgrading capability of a crude oil pipeline for maximum transportation capacity." *Proc., NATC2013, North Africa Technical Conf. and Exhibition 2013*, Vol. 1, Society of Petroleum Engineers, Richardson, TX, 203–219.

American Petroleum Institute (API). (2004). "Specification for line pipe." *API 5L*, Washington, DC.

ASTM. (2011a). "Standard test methods for Rockwell hardness of metallic materials." *E18–11*, West Conshohocken, PA.

ASTM. (2011b). "Standard guide for preparation of metallographic specimens." *E3–11*, West Conshohocken, PA.

ASTM. (2013). "Standard test methods for determining average grain size." *E112–13*, West Conshohocken, PA.

Bolzon, G., Boukharouba, T., Gabetta, G., Elboujdaini, M., and Mellas, M., eds. (2011a). "Corrosion protection of pipelines transporting hydrocarbons." *NATO science for peace and security series C: Environmental security*, Springer, Dordrecht, Netherlands.

Bolzon, G., and Buljak, V. (2011). "An effective computational tool for parametric studies and identification problems in materials mechanics." *Comput. Mech.*, 48(6), 675–687.

Bolzon, G., Buljak, V., Maier, G., and Miller, B. (2011b). "Assessment of elastic–plastic material parameters comparatively by three procedures based on indentation test and inverse analysis." *Inverse Probl. Sci. Eng.*, 19(6), 815–837.

Bolzon, G., Maier, G., and Panico, M. (2004). "Material model calibration by indentation, imprint mapping and inverse analysis." *Int. J. Solids Struct.*, 41(11–12), 2957–2975.

Bolzon, G., Molinas, B., and Talassi, M. (2012). "Mechanical characterization of metals by indentation tests: An experimental verification study for on site applications." *Strain*, 48(6), 517–527.

Bolzon, G., and Talassi, M. (2012). "Model reduction techniques in computational materials mechanics." *Bytes and science*, G. Zavarise and D. P. Boso, eds., CIMNE, Barcelona, Spain, 131–143.

Chen, X., Ogasawara, N., Zhao, M., and Chiba, N. (2007). "On the uniqueness of measuring elastoplastic properties from indentation: The indistinguishable mystical materials." *J. Mech. Phys. Solids*, 55(8), 1618–1660.

De Waard, C., Lotz, U., and Dugstad, D. (1995). "Influence of liquid flow velocity on CO_2 corrosion: A semi-empirical model." *Corrosion/95*, NACE International, Houston, 128.

European Committee for Standardization. (2005). "Metallic materials–Rockwell hardness test—Part 1: Test method (scales A, B, C, D, E, F, G, H, K, N, T)." *EN ISO 6508–1*, Brussels, Belgium.

European Committee for Standardization. (2009). "Metallic materials–Tensile testing—Part 1: Method of test at room temperature." *EN ISO 6892–1*, Brussels, Belgium.

ISO. (1994). "Accuracy (trueness and precision) of measurement methods and results—Part 1: General principles and definitions." *ISO 5725–1*, Geneva, Switzerland.

ISO. (2002). "Metallic materials—Instrumented indentation test for hardness and materials parameters—Part 1: Test method." *ISO 14577–1*, Geneva.

ISO. (2008). "Metallic materials—Measurement of mechanical properties by an instrumented indentation test—Indentation tensile properties." *ISO/TR 29381*, Geneva, Switzerland.

Jang, J. I., et al. (2005a). "Application of instrumented indentation technique for enhanced fitness-for-service assessment of pipeline crack." *Int. J. Fract.*, 131(1), 15–33.

Jang, J. I., Choi, Y., Lee, Y. H., and Kwon, D. (2005b). "Instrumented microindentation studies on long-term aged materials: Work-hardening exponent and yield ratio as new degradation indicators." *Mater. Sci. Eng. A*, 395(1–2), 295–300.

Math Works. (2007). *Matlab, user's guide and optimization toolboxes, release 7.4.0*, Natick, MA.

Molinas, B. J., and Povolo, F. (1992). "Present state of the controversy about the grain relaxation." *Il Nuovo Cimento D*, 14(3), 287–332.

Nykyforchyn, H., Lunarska, E., Tsyrulnyk, O. T., Nikiforov, K., Genarro, M. E., and Gabetta, G. (2010). "Environmentally assisted in-bulk steel degradation of long term service gas trunkline." *Eng. Fail. Anal.*, 17(3), 624–632.

Qian, X., Cao, Y., and Lu, J. (2007). "Dependence of the representative strain on the hardening functions of metallic materials in indentation." *Scr. Mater.*, 57(1), 57–60.

Seok, C. S., and Koo, J. M. (2006). "Evaluation of material degradation of 1Cr–1Mo–0.25V steel by ball indentation and resistivity." *J. Mater. Sci.*, 41(4), 1081–1087.

Simulia Dassault Système. (2009). *ABAQUS/standard, theory and user's manuals, release 6.9*, Providence, RI.

U.S. Environmental Protection Agency. (2006). "Using hot taps for in service pipeline connections." ⟨http://www.epa.gov/gasstar/documents/ll_hottaps.pdf⟩ (Jun. 6, 2013).